

2012년 2월
석사학위논문

Surface Characteristics of
Hydroxyapatite(HA) Coating
on the Dental Implant Alloy
by Pulsed Laser Deposition Methods

조선대학교 대학원

치 의 학 과

신 승 표

Surface Characteristics of
Hydroxyapatite(HA) Coating
on the Dental Implant Alloy
by Pulsed Laser Deposition Methods

펄스레이저 코팅법을 이용한 HA코팅된 치과용
임플란트 합금의 표면특성

2012년 2월 24일

조선대학교 대학원

치 의 학 과

신 승 표

Surface Characteristics of
Hydroxyapatite(HA) Coating
on the Dental Implant Alloy
by Pulsed Laser Deposition Methods

지도교수 정 재 현

이 논문을 치의학 석사학위신청 논문으로 제출함

2011년 10월

조선대학교 대학원

치 의 학 과

신 승 표

신승표의 석사학위 논문을 인준함

위원장 조선대학교 교수 최 한 철 (인)

위 원 조선대학교 교수 정 재 현 (인)

위 원 조선대학교 교수 김 희 중 (인)

2011년 11월

조선대학교 대학원

목 차

국문초록	v
I . INTRODUCTION	1
II . MATERIALS AND METHODS	3
III. RESULTS AND DISCUSSION	5
IV. CONCLUSION	17
REFFENRENCES	18

LIST OF TABLES

Table 1. Corrosion potential (E_{corr}), corrosion current density(I_{corr}), pitting potential(E_{pit}), repassivation potential(E_{rep}) of non-HA coated and HA coated Ti alloy after electrochemical test in 0.9 % NaCl solution at 36.5 ± 1 °C 10

Table 2. Polarization resistance (R_p) and solution resistance of non-HA coated and HA coated Ti alloy in 0.9 % NaCl solution at 36.5 ± 1 °C 16

LIST OF FIGURES

Fig. 1. FE-SEM(a,b), XPS(c) and EDS(d) showing the HA (tooth ash) target surface	4
Fig. 2. FE-SEM and EDS showing the structures and compositions of Ti (a) and Ti-6Al-4V (b) surface	5
Fig. 3. FE-SEM and EDS showing the HA coating morphologies and compositions on the Ti (a, b) and Ti-6Al-4V (c, d) surface	7
Fig. 4. XRD peaks of non-HA coated and HA coated Ti and Ti-6Al-4V surface	8
Fig. 5. Cyclic potentiodynamic polarization curves of non-HA coated and HA coated Ti alloy after CPP test in 0.9 % NaCl solution at 36.5±1 °C	10
Fig. 6. FE-SEM and EDS showing the corrosion morphologies of non-HA coated and HA coated Ti alloy after CPP test in 0.9 % NaCl solution at 36.5±1 °C. (a) non-HA coated Cp-Ti, (b) HA coated Cp-Ti, (c) non-HA coated Ti-6Al-4V, and (d) HA coated Ti-6Al-4V	12
Fig. 7. Current-time curves of non-HA coated and HA coated Ti alloy after potentiostatic test at constant potential (300mV) in 0.9 % NaCl solution at 36.5±1 °C	13

Fig. 8. FE-SEM and EDS showing the corrosion morphologies of HA coated Cp-Ti (a, b) and Ti-6Al-4V(c, d) after potentiostatic test at constant potential (300mV) in 0.9 % NaCl solution at 36.5±1 °C 14

Fig. 9. Bode plots of non-HA coated and HA coated Ti alloy after AC impedance test in 0.9 % NaCl solution at 36.5±1 °C 16

국문초록

펄스레이저 코팅법을 이용한 HA코팅된 치과용 임플란트 합금의 표면특성

신 승 표

지도교수 : 정재현, 치의학박사

치의학과

조선대학교 대학원

본 연구는 치과용 임플란트 합금의 표면에 펄스레이저를 이용하여 hydroxyapatite(HA)를 코팅한 후 표면특성을 조사한 것이다.

HA는 치아회분말을 이용하여 Cp-Ti의 Ti-6Al-4V 합금 기판에 600 °C에서 60분 동안 성장을 시켰으며 산소의 압력을 5×10^{-3} - 5×10^{-1} Torr 범위로 하여 코팅하였다. 펄스화된 KrF excimer laser (248nm, 30ns duration)를 사용하였으며 반복속도는 5Hz로 하였다. 레이저 빔의 에너지를 일반적으로 사용하는 130mJ/pulse로 하여 실험을 하였다. 코팅막의 형상, 화학조성, 결정구조는 field-emission scanning electron microscopy(FE-SEM), energy dispersive x-ray spectroscopy(EDS), x-ray diffraction(XRD)을 이용하여 조사하였다. 전기화학적 거동은 potentiostat (2273, EG&G, USA)을 이용하여 0.9% NaCl용액에서 양극분극곡선과 임피던스분석을 하여 조사하였다.

이상과 같은 실험을 통하여 다음과 같은 결론을 얻었다.

1. Ti-6Al-4V합금의 조직은 α 와 β 상을 보였고 침상의 조직을 보인 반면, Cp-Ti는 α 상을 갖는 등축구조를 보였다.
2. HA코팅된 표면의 형상은 1-2 μm 입자로 구성되었으며 알갱이와 같은 입자들이 표면에 분포되었다.
3. 치과용 임플란트 합금에 PLD법으로 코팅된 HA막은 우수한 내식성을 보였다. 따라서 PLD법으로 코팅된 HA표면은 치과용 임플란트 표면에 적용이 가능하며 생체적합성을 개선할 수 있는 표면처리법으로 평가되었다.

I. INTRODUCTION

Many surface preparation processes have been developed in order to improve the functional structures and performances of dental materials through surface modification. Physical vapor deposition (PVD) including ion plating, ion beam enhanced deposition (IBED), ion implantation, plasma spray, electron beam PVD (EB-PVD), sputtering, and pulsed laser deposition (PLD) [1-3] is used to improve the functionality, wear-resistance, corrosion-resistance, and oxidation-resistance of various materials. Regarding as, among the coating techniques, the plasma spraying method is the most commonly used for HA coating of dental implant, which include poor coating morphology, change of substrate due to high temperature of coating process, and low adhesion strength after clinical use. For this problem, the PLD is used for formation of the HA film with high density and bonding strength between HA film and substrate.

PLD is a new method to deposit HA thin films on various metallic substrates for biomaterials. The improvement in the surface coating of implant materials is necessary because some specific industries and biomaterial field require the metallic biomaterials with corrosion resistance, oxidation resistance, and wear resistance. For instance, HA is coated on the surface of dental implant materials or orthopedic materials for osseointegration between bone and implant interface. The HA coated film can be expected to have a good osseointegration to bone after implantation [4].

PLD is used to coat metals and nonmetals (ceramics) of periodic table, and many researchers are studying on it, like an EB-PVD [5], a critical process of coating, is a method in which vaporized materials are coated on substrates. Several researchers including us reported that when HA film are

coated by EB-PVD, HA coating showed the higher corrosion resistance [2] and can increase the biocompatibility of the EB-PVD coated surface compared to TiN coated surface. Also, HA coating by EB-PVD is reported to be superior in corrosion resistance [2]. However, the surface properties of HA film coated by PLD on Ti alloy for dental implant materials have rarely been studied by some researchers.

In this study, we investigated the surface characteristics of hydroxyapatite(HA) coating on the dental implant alloy by pulsed laser deposition methods.

II. MATERIALS AND METHODS

In this work, tooth ash of HA source was prepared with consisted of Ca and P(Ca/P=1.67) as shown in Fig. 1. Fig. 1(a) and (b) show the surface of HA (tooth ash) target after sintering. The particles of HA was combined by sintering as shown in Fig. 1(b), and the composition was confirmed by X-ray photoelectron spectroscopy(XPS) and energy dispersive X-ray spectroscopy(EDS) analysis as shown in Fig. 1(c) and (d), respectively.

The HA coatings were performed by PLD. The HA (tooth ash) films were grown on Cp-Ti and Ti-6Al-4V alloy substrates at 600 °C for 60min under different O₂ pressures ranging from 5×10^{-3} to 5×10^{-1} Torr. Before being loaded into the growth chamber, the substrates were cleaned in an ultrasonic bath using trichloroethylene, acetone and ethanol, in sequence. The growth chamber was pumped down to a base pressure of 5×10^{-6} Torr prior to back filling it with the O₂ ambient. A pulsed KrF excimer laser(248nm, 30ns duration) operated with the repetition rate of 5Hz was used. The laser beam energy was typically set at 130mJ/pulse. Film surface topology, chemical composition, and phase and crystal structure were determined using field emission scanning electron microscopy(FE-SEM), EDS, and X-ray diffractometer (XRD, X'pert PRO, Philips) with Cu K α radiation.

Electrochemical behaviors were investigated by potentiostat (PARSTAT 2273, EG&G, USA). A standard three-electrode cell having the specimen as a working electrode and a high-carbon counter electrode were used. The potential of the working electrode was measured against a saturated calomel electrode (SCE) and all specimen potentials were referenced to this electrode.

The corrosion behavior of coated sample was observed by a

potentiodynamic method (potential range from -1000 to 1500 mV) at scan rate of 1.67 mV/s in 0.9% NaCl solution at 36.5 ± 1 °C and potentiostatic method at constant potential (300 mV). Also, AC impedance test was performed from 10 m Hz to 100 kHz in 0.9% NaCl solution at 36.5 ± 1 °C. An equivalent circuit was assigned for the acquired data and the data were curve fitted using ZSimpWin software. After corrosion test, the corrosion morphologies were observed by FE-SEM and EDS.

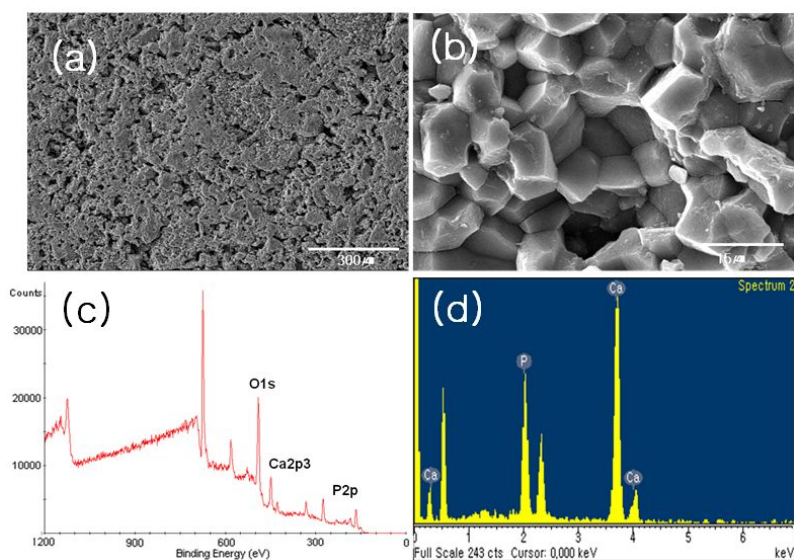


Fig. 1. FE-SEM(a,b), XPS(c) and EDS(d) showing the HA (tooth ash) target surface.

III. RESULTS AND DISCUSSION

1. The surface morphology of HA coated film

Fig. 2 shows the FE-SEM and EDS of Cp-Ti and Ti-6Al-4V alloy. In the case of Cp-Ti, α -phase was formed in the matrix, whereas in case of Ti-6Al-4V alloys, α - β structure formed in the grain like a needle or acicular shape [6]. From our pre-research paper [7], the Ti-6Al-4V alloy possessed a two-phase, α + β structure, due to presence of vanadium (β -phase stabilizer) and aluminum (an α -phase stabilizer). These phases were composed of needle-like structure as shown in Fig. 2(b). As a result of EDS, chemical composition was in accord with alloys design such as Ti, Al, and V element detection.

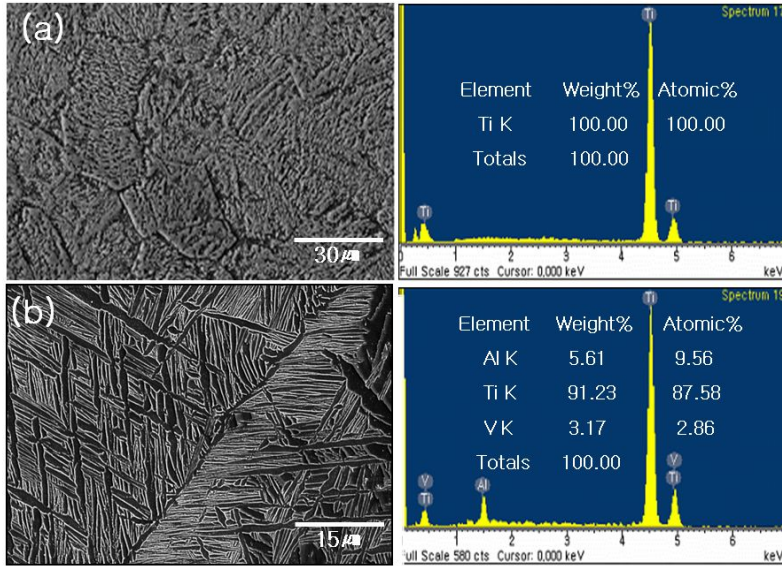


Fig. 2. FE-SEM and EDS showing the structures and compositions of Ti (a) and Ti-6Al-4V (b) surface

Fig. 3 shows the surface morphology and EDS peaks of HA coated Cp-Ti and Ti-6Al-4V alloy after pulsed laser deposition. Fig. 3(a) and (c) showed the HA coated surface with several spherical particles on the surface like a droplet and the coated surface consisted of Ca, P, and Ti from EDS peaks. From the Fig. 3(b) and (d) of high resolution image of Fig. 3 (a) and (c), HA coated surface consists of 1-2 μm droplets and small granular particles. The morphology of the droplets suggests that they may be a result of target splashing [8], since the droplet diameter is much smaller than the particle size of the powder used to prepare the HA target as shown in Fig. 1. The irregular-formed craters and micro particles as shown in the Fig. 3(a) and (c) are formed during vapor deposition, and are considered to be the defects induced by the formation of micro droplets. In particular, the HA deposited layer showed the columnar structure grown at perpendicular direction to the surface [3]. This is because the deposited film was grown toward the direction in which the surface energy was the lowest to grow like a preferred direction, and the growth pattern was shown in the direction of HA (112) and HA (202) [9]. In the case of preferred film growth, the dense film was formed in the coating layer. The growth direction is changed by the factors of the deposition process including the substrate temperature, the speed of deposition, and matrix [10-11]. Therefore, directional growth can increase the corrosion resistance and wear resistance of the surface coating layer, whereas the most severe defects such as micro-bubbles and cracks during deposition can play a role of corrosion site[4].

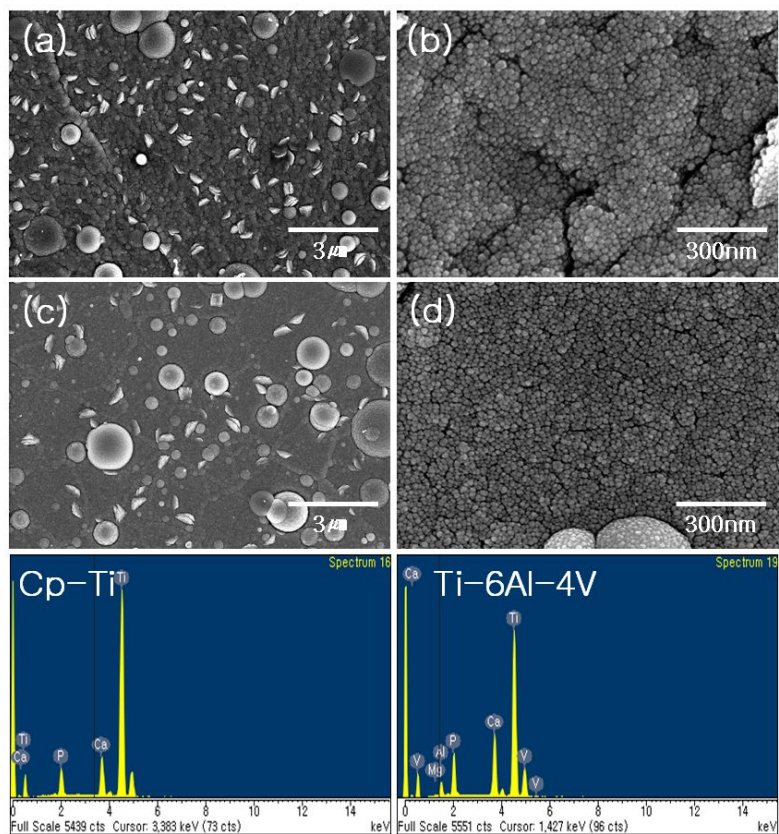


Fig. 3. FE-SEM and EDS showing the HA coating morphologies and compositions on the Ti (a, b) and Ti-6Al-4V (c, d) surface.

Fig. 4 shows the X-ray diffraction profiles of Cp-Ti, Ti-6Al-4V, HA coated Cp-Ti, and HA coated Ti-6Al-4V alloys. The peaks were indexed using the JCPDS diffraction data of Ti-alloys. In the case of Cp-Ti, (100), (002) and (101) peaks showed the α -phase. The Ti-6Al-4V alloy possessed a two-phase α - β structure due to presence of vanadium (β -phase stabilizer) and aluminum (α -phase stabilizer). Ti-6Al-4V alloy revealed the presence of (101) $_{\beta}$ peak in addition to those previously associated with the metastable β -phase. It is reported in the literature that the amount of α'' -phase increases with increasing cooling rate due to the transformation of β -phase into α'' [12-13]. These phases were composed of needle-like structure as shown in Fig. 2.

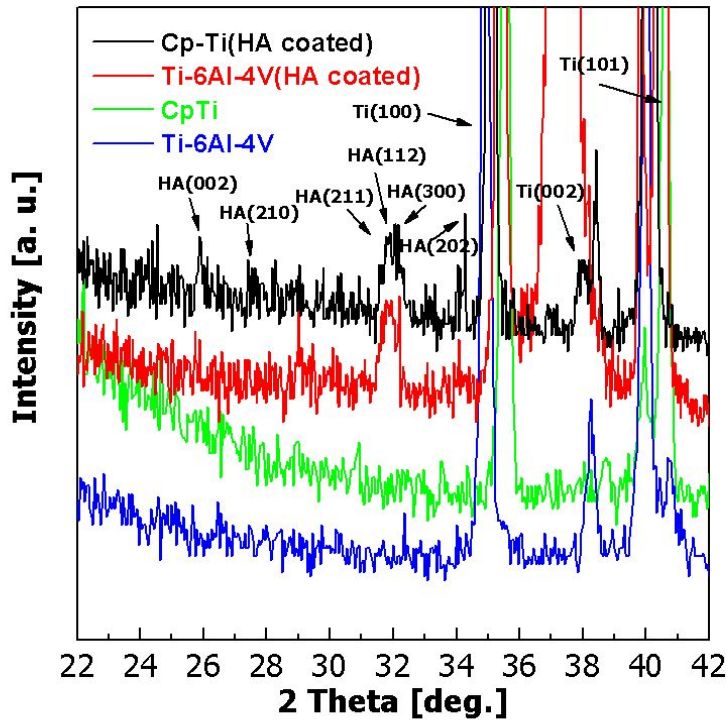


Fig. 4. XRD peaks of non-HA coated and HA coated Ti and Ti-6Al-4V surface.

2. DC corrosion behavior of HA coated film

Fig. 5 shows the results of the corrosion test in 0.9% NaCl in order to investigate the effect of HA films on the cyclic potentiodynamic polarization curve (CPP). This method is used for estimation of pitting resistance. From the CPP curves, CPP curves of HA coated surface shifted to left side compared to non-coated surface. It was thought that HA coated surface of Ti-6Al-4V alloy is superior to any other cases in corrosion resistance because the HA thin film including the oxidation film such as TiO_2 was formed on the surface to increase the corrosion resistance[2-3]. In particular, the unstable region of anodic polarization curve showed on the surface of non-coated samples. It is confirmed that coated substances are sufficiently protected by HA film against Cl^- ions on the surface [4]. From the CPP curves, the pitting potential (E_{pit}) was 1060mV for Cp-Ti, and 1540 mV for Ti-6Al-4V alloy, whereas, 1350mV for HA coated Cp-Ti, and 1580 mV for HA coated Ti-6Al-4V alloy. The E_{pit} of HA coated samples increased compared to non-HA coated samples. It is confirmed that the HA layer inhibits the Cl^- attack to increase the corrosion resistance [2,3,14]. The corrosion parameters obtained from the CPPT measurements, including E_{corr} , $I_{300\text{mV}}$, I_{corr} and I_{pass} are summarized in Table 1.

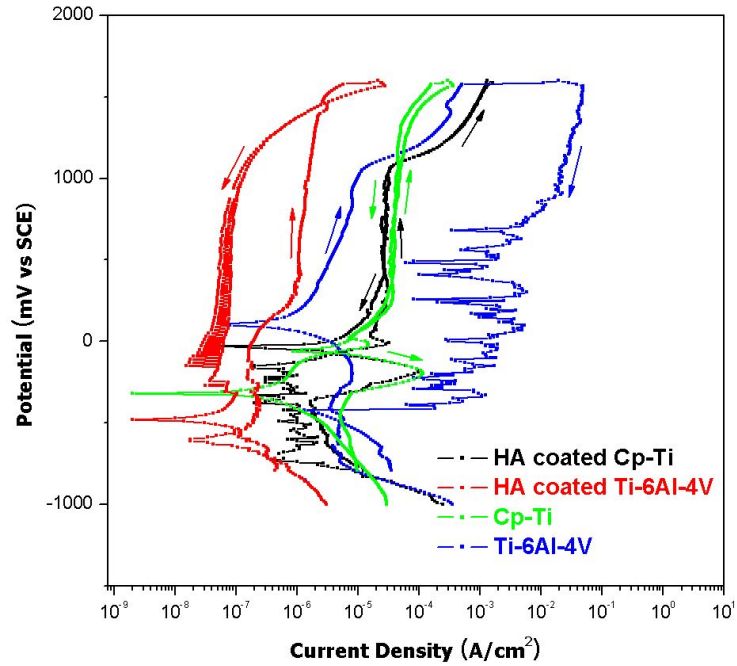


Fig. 5. Cyclic potentiodynamic polarization curves of non-HA coated and HA coated Ti alloy after CPP test in 0.9 % NaCl solution at 36.5 ± 1 °C.

Table 1. Corrosion potential (E_{corr}), corrosion current density (I_{corr}), pitting potential (E_{pit}), repassivation potential (E_{rep}) of non-HA coated and HA coated Ti alloy after electrochemical test in 0.9 % NaCl solution at 36.5 ± 1 °C.

Data	Non Coated		HA Coated	
	Cp-Ti	Ti-6Al-4V	Cp-Ti	Ti-6Al-4V
$I_{300\text{mV}} (\text{A}/\text{cm}^2)$	2.96×10^{-5}	1.98×10^{-6}	3.78×10^{-5}	9.30×10^{-7}
$E_{\text{corr}} (\text{mV})$	-160	110	-320	-610
$E_{\text{pit}} (\text{mV})$	1060	1540	1350	1580
$E_{\text{rep}} (\text{mV})$	-	-	-	1460
$ E_{\text{pit}} - E_{\text{corr}} $	1220	1430	1670	2190

Fig. 6 shows the corrosion morphologies of non HA coated and HA coated surface after the CPP test. A lot of corrosion products and destroyed HA film particles showed on the surface of the coated film. It is considered to be produced by corrosion of coating substances in the 0.9% NaCl solution. EDS peaks mainly consisted of Ca, Ti, O, and P, which may be induced by Cl^- . As shown in Fig. 6, the corrosion morphology of HA showed some cracks and corrosion products on the surface. The most severe defect during deposition was micro-bubbles, droplets and cracks, and these defects serve as important factors for corrosion resistance because the defects were easily dissolved when it exposed to the corrosive oral environment in the case of dental implant [2-3], The corrosion along the coating layer can reduce the durability of the dental implants after clinical use.

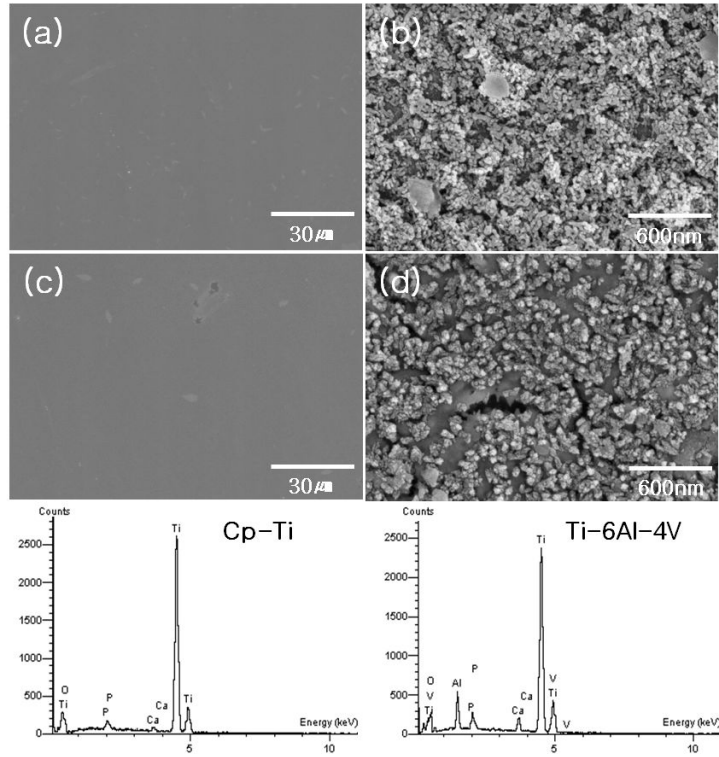


Fig. 6. FE-SEM and EDS showing the corrosion morphologies of non-HA coated and HA coated Ti alloy after CPP test in 0.9 % NaCl solution at 36.5 ± 1 °C. (a) non-HA coated Cp-Ti, (b) HA coated Cp-Ti, (c) non-HA coated Ti-6Al-4V, and (d) HA coated Ti-6Al-4V.

Fig. 7 shows the current-time curves of non-HA coated and HA coated surface after the potentiostatic test at 300mV for durability of passive film and HA coated film. The current density of the all samples decreased with time, but HA coated samples showed the lower current density than non-HA coated samples due to stable film formation on the surface[2]. After test of HA coated film stability, surface morphology showed the some pits at around the droplets as shown in Fig. 8. It was thought that the boundary between droplet and coated surface acted on aggressive site in the NaCl solution, and then boundary was continuously dissolved. Finally, pits were formed as shown in Fig. 8(c). From the EDS results, Ti, Al, O, Ca, and P peaks were detected from surface due to corrosion products come from dissolved hydroxyapatite and formation of oxidation film such as Al_2O_3 and TiO_2 [2-3].

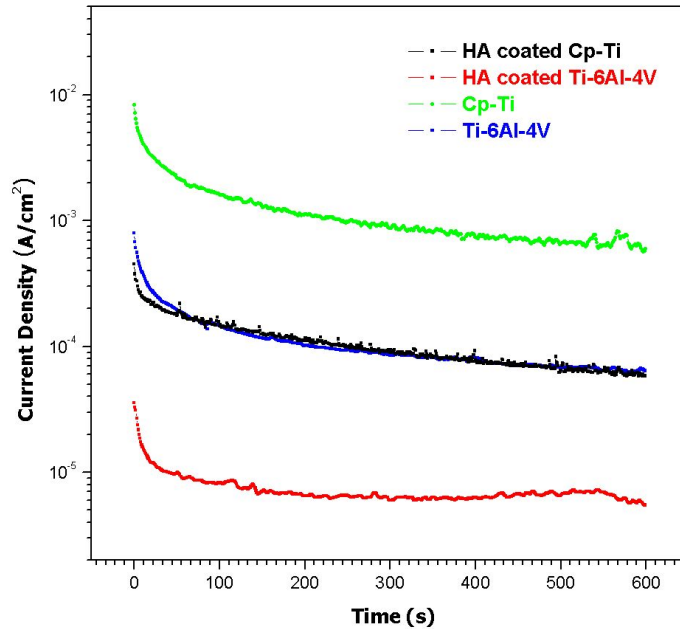


Fig. 7. Current-time curves of non-HA coated and HA coated Ti alloy after potentiostatic test at constant potential (300mV) in 0.9 % NaCl solution at 36.5 ± 1 °C.

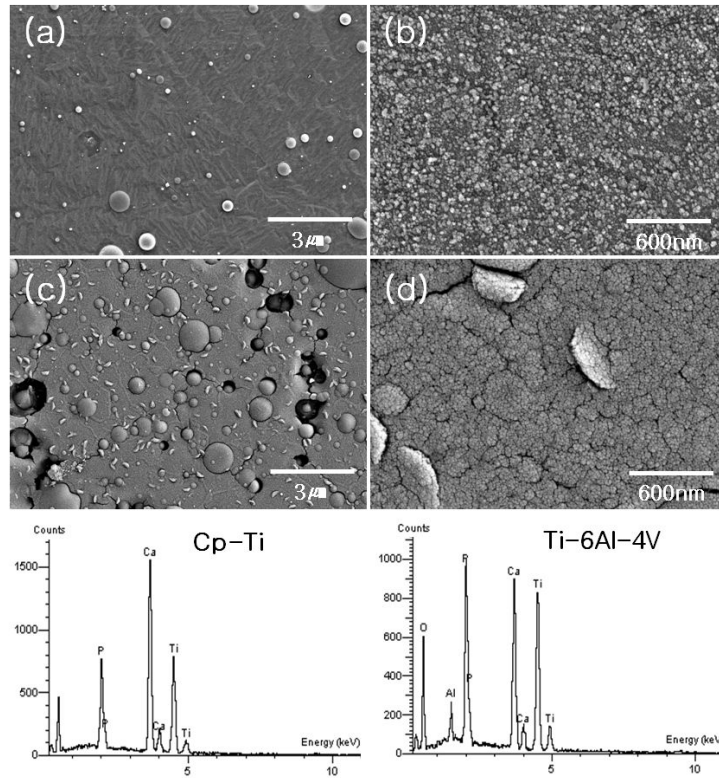


Fig. 8. FE-SEM and EDS showing the corrosion morphologies of HA coated Cp-Ti (a, b) and Ti-6Al-4V(c, d) after potentiostatic test at constant potential (300mV) in 0.9 % NaCl solution at 36.5 ± 1 °C.

3. AC impedance behavior of HA coated film

Fig. 9 shows the Bode plots of non-HA coated and HA coated Cp-Ti and Ti-6Al-4V alloy after AC impedance test in 0.9 % NaCl solution at 36.5 ± 1 °C. According to the results of AC impedance, polarization resistance of HA coated samples showed the higher than that of non-HA coated samples, as shown in Table 2, the HA film and oxide film that was formed on the surface by Ti and Al increases corrosion resistance in the NaCl solution [4].

Impedance measurements were carried out after 30 min of initial immersion in the electrolyte. A high impedance value (R_p) of the order of $10^5 - 10^6 \Omega \text{cm}^2$ was obtained at low and medium frequencies, suggesting good corrosion resistance for HA coated Ti-6Al-4V alloy surface compared with non-coated alloy. R_s represents the solution resistance. A higher value of R_p implies higher corrosion resistance [2,15]. The electrochemical studies suggested that the surface after HA coating possesses good corrosion resistance with an enhanced protection against Cl^- ion attacks[3].

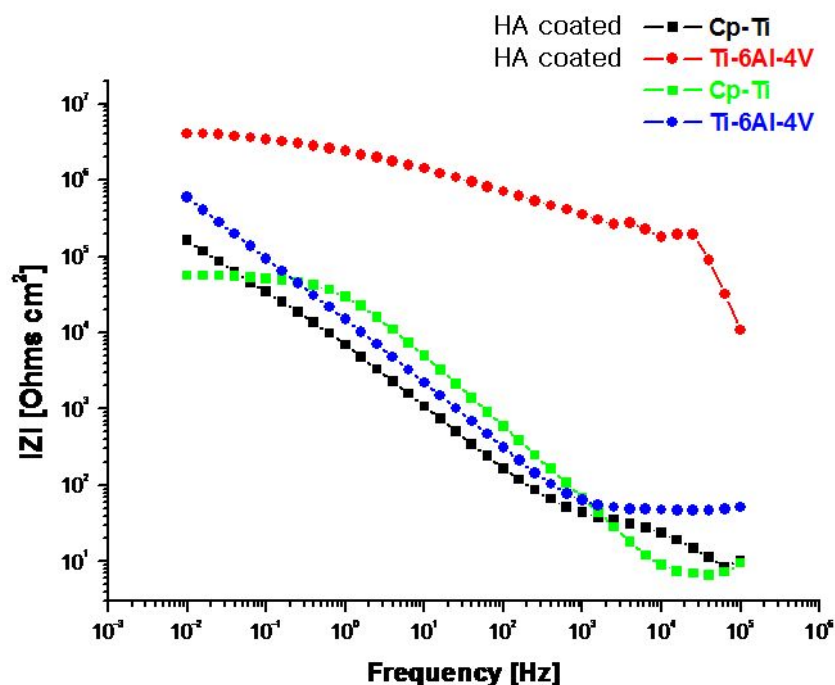


Fig. 9. Bode plots of non-HA coated and HA coated Ti alloy after AC impedance test in 0.9 % NaCl solution at 36.5 ± 1 °C.

Table 2. Polarization resistance (R_p) and solution resistance of non-HA coated and HA coated Ti alloy in 0.9 % NaCl solution at 36.5 ± 1 °C.

Non-coated	Cp-Ti	Ti-6Al-4V	HA Coated	Cp-Ti	Ti-6Al-4V
$R_p (\Omega cm^2)$	5.57×10^4	3.24×10^6	$R_p (\Omega cm^2)$	1.62×10^5	4.03×10^6
$R_\Omega (\Omega cm^2)$	18.24	8.80	$R_\Omega (\Omega cm^2)$	20.86	48.82

IV. CONCLUSIONS

To investigate the surface characteristics of hydroxyapatite(HA) coating on the dental implant alloy, pulsed laser deposition method was used for HA coating and then, corrosion test were carried out using potentiostat.

The experimental results are as follows;

1. The microstructures of Ti-6Al-4V showed α and β phase with needle-like, and Cp-Ti had the α phase with equiaxed structure.
2. The HA coated morphology consisted of 1-2 μm droplets and grain-like particles.
3. The pitting potential (E_{pit}) was 1060mV for Cp-Ti, and 1540 mV for Ti-6Al-4V alloy, whereas, 1350mV for HA coated Cp-Ti, and 1580 mV for HA coated Ti-6Al-4V alloy.
4. The HA coated samples showed the lower current density than non-HA coated samples due to stable film formation on the surface.
5. From the results of AC impedance, polarization resistance of HA coated samples showed the higher than that of non-HA coated samples. The HA films deposited alloys by PLD were good corrosion resistance against Cl^- ion-likehalides.

It is considered that the dental implant surface can be improved by HA coating with PLD methods.

REFERENCES

- [1] H. C. Choe, Y. M. Ko and K. Y. Hwang, J. of the Japan Institute of Metals., 65 (2001) 253.
- [2] Y. H. Jeong, H. C. Choe, S. W. Eun, Thin Solid Films 519 (2011) 7050.
- [3] W. G. Kim, H. C. Choe, Thin Solid Films 519 (2011) 7045.
- [4] Y. H. Jeong, W. G. Kim, G. H. Park, H. C. Choe, Y. M. Ko, Trans. Nonferrous Met. Soc. China 19 (2009) 852.
- [5] S. Schiller, U. Heisig and S. Panzer, Electron Beam Technology, John Wiley and Sons, Inc. (1982) 25.
- [6] W. G. Kim, H. C. Choe, Y. M. Ko, W. A. Brantley, Thin Solid Films 517 (2009) 5033.
- [7] K. Lee, H. C. Choe, B. H. Kim, Y. M. Ko, Surface and Coating Technol., 205 (2010) S267.
- [8] F. X. Rong, Liquid Target Pulsed-Laser Deposition. Applied Physics Letters 67 (1995) 1022.
- [9] J. C. Knight and T. F. Page, Thin Solid Films, 193/194 (1990) 431.
- [10] A. Deblanc Bauer, M. Herranen, H. Ljungcrantz, J-O.Carlsson, J-E. Sundgren, Surface and Coating Technol., 91(1997) 208.
- [11] J. Takadoun, H. H. Bennami, Surface and Coating Technol., 96 (1997) 272.
- [12] L. H. Li, Y. M. Kong, H. W. Kim, Y. W. Kim, S. J. Seo, J. Y. Koak, Biomaterials 25 (2004) 2867.
- [13] H. W. Kim, Y. H. Koh, L. H. Li, S. Lee, H. E. Kim, Biomaterials 25 (2004) 2533.
- [14] M. H. Fathi, M. Salehi, A. Saatchi, V. Mortazavi, S. B. Moosavi, Dental Materials, 19 (2003) 188.
- [15] V. S. Saji, H. C. Choe, Corrs. Sci., 51 (2009) 1658.